Unbinding transitions and phase separation of multicomponent membranes

Thomas R. Weikl, Roland R. Netz, and Reinhard Lipowsky

MPI für Kolloid- und Grenzflächenforschung, Am Mühlenberg, 14476 Golm, Germany

(Received 4 August 1999)

Multicomponent membranes in contact with another surface or wall are studied by a variety of theoretical methods and Monte Carlo simulations. The membranes contain adhesion molecules which are attracted to the wall and, thus, act as local stickers. It is shown that this system undergoes lateral phase separation leading to discontinuous unbinding transitions if the adhesion molecules are larger than the nonadhesive membrane components. This process is driven by an effective line tension which depends on the size of the stickers and arises from the interplay of shape fluctuations and sticker clusters.

PACS number(s): 87.16.Dg, 64.75.+g, 83.70.Hq

Biomembranes contain a large number of different components, lipids, and membrane proteins, which are organized in a rather complex fashion. Various aspects of this self-organization can be studied in biomimetic systems such as multicomponent bilayers. One such aspect is the interplay of membrane composition and shape; for a review, see [1]. Another aspect is the interplay of membrane composition and adhesion which will be addressed here.

A multicomponent membrane represents a two-dimensional system which can undergo lateral phase separation and, thus, exhibit coexistence regions of several thermodynamic phases [2]. Since biomembranes are maintained in their fluid state by sterols such as cholesterol or by unsaturated bonds in the lipid chains, we will study multicomponent membranes which exhibit several fluid phases. Examples are provided by several mixtures such as dielaidoyl PC and dipalmitoyl PE [3], phospholipid and cholesterol [4–7], and palmitoyl oleyl phoshatidyl serine (POPS) and didodecenoyl PC [8].

The adhesion of biomembranes, which is responsible for cell-cell adhesion and for many cell signaling processes, is governed by the interplay of generic repulsive forces and specific attractive forces. The latter forces are mediated by adhesion molecules (cell-cell adhesion) or receptor and ligand pairs (cell signaling) which represent anchored membrane proteins and which play the role of local stickers. We will mimic this situation by multicomponent membranes with one adhesive component which is attracted towards another surface or ''wall.'' In general, the adhesive behavior is now determined by the interplay of (i) *trans*-interactions, as mediated by the stickers between the two surfaces, and of (ii) *cis*-interactions between two stickers anchored to the same membrane. This interplay was recently studied [9,10] in the framework of theoretical models, which describe both the membrane shape and the local membrane composition, and it was shown that small stickers with purely repulsive cis-interactions lead to a continuous unbinding transition without lateral phase separation.

In this Rapid Communication, we report some surprising changes in the membrane behavior as soon as the size of the adhesion molecules exceeds the size of the other nonadhesive membrane components. Such size differences are relevant for biomembranes since the adhesive membrane proteins are indeed large compared to the various lipid components. In such a situation, the membrane is found to *undergo lateral phase separation and, thus, discontinuous unbinding transitions even if the cis-interactions between the stickers are purely repulsive*. This is illustrated in Figs. 1(a) and 1(b) which display typical configurations of the adhesion molecules as observed in Monte Carlo (MC) simulations. In these two figures, the adhesion molecules cover the same area as 2×2 and 3×3 nonadhesive molecules, respectively. As explained further below, this behavior can be understood in terms of an *effective line tension arising from the interplay between shape fluctuations of the membrane and cluster formation of the stickers*.

Some model systems consisting of lipid membranes and sticker molecules have been investigated experimentally; examples are (i) membranes containing cationic lipids in contact with a negatively charged surface [11], and (ii) membranes with biotinylated lipids which are bound to another biotinylated surface via streptavidin [12]. In both systems, lateral phase separation has been observed. In addition, the adhesion of neurons to stepped surfaces has also been studied quite recently [13]. In this latter case, the contact area appears to be rather flat, a situation which presumably indicates that the membrane experiences a relatively large lateral tension. In the following, we will focus on the case where the membranes are essentially tensionless in order to eliminate one parameter from the problem. However, the underlying line tension mechanism, which we explain next, is general and also effective for membranes under lateral tension.

In order to understand the behavior shown in Figs. 1(a) and 1(b), let us consider an arbitrary shape of the adhering membrane, and let us divide the membrane surface into two types of domains: (i) ''Bound domains'' corresponding to all membrane segments with a separation from the wall which is smaller than the potential range l_v of the attractive sticker potential, and (ii) ''Unbound domains'' corresponding to all membrane segments which have a separation which exceeds l_v. These two types of domains are separated by ''domain boundaries,'' where the membrane-wall separation is equal to l_v. The membrane surface consisting of these two types of domains is now decorated with stickers. Obviously, in order to gain more adhesive energy one has to place more stickers into the bound domains.

If these stickers have the same size as the nonadhesive molecules, the maximal adhesive energy, which one can ob-
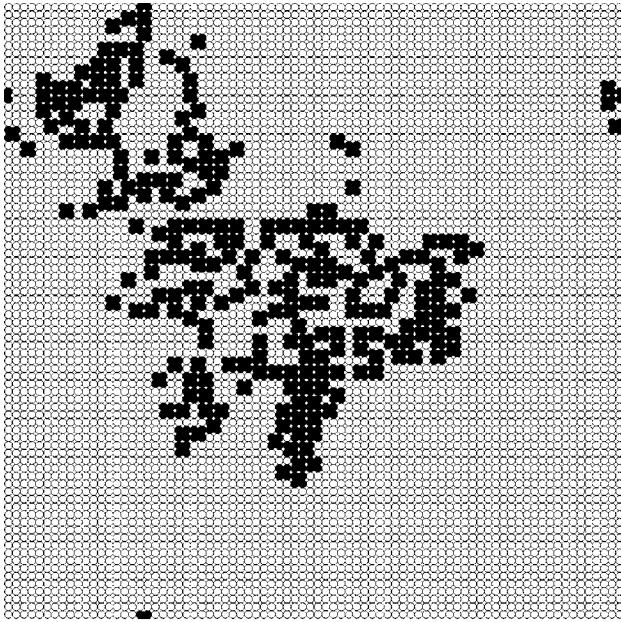
(a)
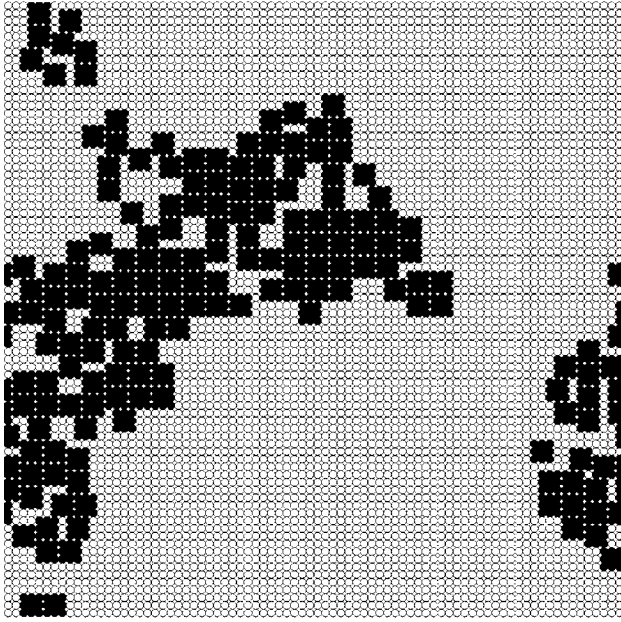
(b)

FIG. 1. Multicomponent membranes with stickers (black) which exceed the size of the nonadhesive molecules (white): Both (a) 2×2 stickers and (b) 3×3 stickers phase separate within the adhering membrane even though these stickers do not experience any attractive *cis*-interactions.

tain in this way, depends only on the total area of the bound domains but is independent (i) of the number of bound domains and (ii) of the shape of these domains. In contrast, if we cover the area of the bound domains with Q-stickers and $Q > 1$, many of these stickers will sit on the domain boundaries and thus will not contribute to the adhesive energy in the same way as those in the interior of the bound domains. Therefore, the boundaries between the bound and unbound domains are characterized by an effective line tension which favors the aggregation of the bound domains, i.e., phase separation provided one has $Q > 1$.

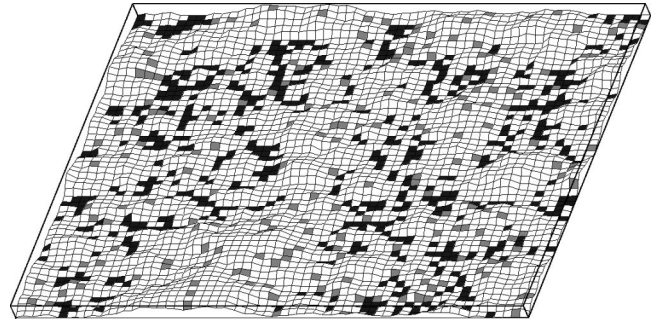A systematic theory for a multicomponent membrane

FIG. 2. Typical Monte Carlo configuration of an adhering membrane with 1×1 stickers. Bound stickers are black, unbound stickers grey, and nonadhesive molecules are white. Bound stickers have some tendency to cluster but the membrane does *not* phase separate in the absence of attractive *cis*-interactions.

with anchored stickers in contact with a wall or substrate must include a field l for the local separation between the membrane and the wall and a concentration field n of the stickers. It is convenient to discretize the space into a two-dimensional square lattice with lattice constant a and lattice sites i. The sticker positions can then be described by occupation numbers $n_i = 0,1$ and the membrane separation by $l = l_i \geq 0$. In terms of these variables, the grand canonical Hamiltonian has the general form

$$H\{l,n\} = H_{el}\{l\} + \sum_i n_i[V_i(l) - \mu] + \sum_{\langle ij \rangle} W_{ij} n_i n_j, \quad (1)$$

where $\langle ij \rangle$ indicates a summation over all pairs of lattice sites with $i \neq j$. For an oriented membrane the elastic term has the form $H_{el} = \Sigma_i (\kappa/2a^2)(\Delta_d l_i)^2$ with $\Delta_d l_i = \Delta_d l_{x,y} = l_{x+a,y} + l_{x-a,y} + l_{x,y+a} + l_{x,y-a} - 4l_{x,y}$. The potential $V_i(l)$ represents the adhesion potential of an individual sticker at lattice site i, the parameter μ is the chemical potential for the stickers and W_{ij} the cis-interaction energy between two stickers at sites i and j.

In the case of 1×1 stickers with the size of one lattice site, we consider the square-well adhesion potential

$$V_i(l) = V(l_i) = U\theta(l_v - l_i) \quad (2)$$

with $\theta(x) = 0$ for $x < 0$ and $\theta(x) = 1$ for $x \geq 0$, which is characterized by the binding energy $U < 0$ and the potential range l_v. Such a potential applies, e.g., to lipids with sticky headgroups. The *cis*-interactions are taken to be zero for all lattice sites i and j. By introducing the rescaled field $z \equiv (l/a)\sqrt{\kappa/T}$, the number of parameters can be reduced to the dimensionless quantities U/T, μ/T, and the rescaled potential range $z_v \equiv (l_v/a)\sqrt{\kappa/T}$.

In Fig. 2, we see a snapshot from a Monte Carlo (MC) simulation. Bound stickers are black, unbound stickers gray. Even in the absence of attractive *cis*-interactions W_{ij}, bound stickers have a tendency to form small clusters arising from attractive entropic interactions induced by membrane fluctuations. For an isolated pair of bound stickers, the strength of this interaction has been estimated in Ref. [14]. For a correct treatment of our multisticker system, where screening effects and/or many-sticker interactions are important, we
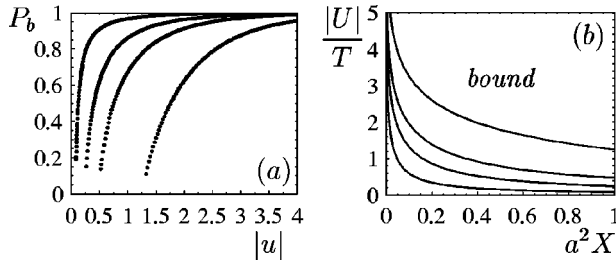
FIG. 3. (a) Contact probability P_b of a *homogeneous* membrane as a function of the depth $|u|$ of the square-well potential for the rescaled potential ranges $z_v = 1$, 0.5, 0.3, and 0.1 (from left to right); (b) Reduced potential depth $|U|/T$ vs sticker concentration X for the continuous unbinding transitions with $z_v = 1$, 0.5, 0.3, and 0.1 (bottom to top).

first sum out the sticker degrees of freedom. The partition function $\mathcal{Z}$ then has the exact form

$$\frac{\mathcal{Z}}{\mathcal{Z}_o^N} = \left[\prod_i \int_0^\infty dl_i \right] e^{-[H_{el}\{l\} + \sum_i V_{ef}(l_i)]/T}, \quad (3)$$

with $\mathcal{Z}_o = 1 + e^{\mu/T}$ and an effective potential $V_{ef}(l_i) = -T \ln[(1 + e^{[\mu - V(l_i)]/T})/(1 + e^{\mu/T})]$, where N denotes the number of lattice sites. The effective potential $V_{ef}(l_i)$ is a square-well potential with range l_v and depth $Tu \equiv -T \ln[(1 + e^{[\mu - U]/T})/(1 + e^{\mu/T})]$. Apart from the prefactor, the partition function (3) now depends only on two parameters, the dimensionless potential depth u and the rescaled potential range $z_v = (l_v/a)\sqrt{\kappa/T}$.

The free energy per unit area $F = -(T/A)\ln \mathcal{Z}$ can be obtained from the contact probability $P_b \equiv \langle \theta(z_v - z_i) \rangle$ since $NP_b = -\partial \ln \mathcal{Z}/\partial u$. The expectation value $\langle \theta(z_v - z_i) \rangle$ can be directly determined from the MC simulations; see Fig. 3(a), and represents the fraction of bound membrane segments, i.e., membrane segments with $z_i < z_v$. The unbinding transition of a homogeneous membrane in a square-well potential is continuous [15]. Since $P_b \sim (u - u_*)$ close to the critical potential depth u_*, we determine u_* by linear extrapolation to $P_b = 0$, where the correlation length and relaxation time of the simulations diverge. The free energy is then given by

$$F = -\frac{T}{a^2} \ln[1 + e^{\mu/T}] + F_{ub} - \frac{T}{a^2} \int_u^{u_*} du' P_b(u'), \quad (4)$$

where F_{ub} denotes the free energy of the unbound membrane associated with the shape fluctuations [16]. The sticker concentration $X = -(\partial F/\partial \mu) = \langle n_i \rangle$ then follows as

$$X = \frac{1}{a^2} \left[(1 - P_b)\frac{e^{\mu/T}}{1 + e^{\mu/T}} + P_b \frac{e^{[\mu - U]/T}}{1 + e^{[\mu - U]/T}} \right]. \quad (5)$$

At the continuous unbinding point, the contact probability P_b vanishes and the chemical potential μ_* is determined by the equation $u_* = u(\mu_*)$. Figure 3(b) shows the resulting unbinding lines in the $(a^2 X, |U|/T)$ plane for several values of z_v. At low sticker concentration X or low binding energy $|U|$, the membrane is unbound. Note that there is no lateral

phase separation in the multicomponent membrane for $W_{ij} = 0$ in agreement with Ref. [9].

Now, let us consider stickers which occupy Q lattice sites. In general, the shape of these stickers may vary but we will focus on the simplest shape corresponding to ''square'' stickers with linear dimension $\sqrt{Q}$. We study two adhesion potentials, the *sum* potential

$$V_i(l) = V(l_{i,1}, \ldots, l_{i,Q}) = U \sum_{q=1}^Q \theta(l_v - l_{i,q}), \quad (6)$$

where $\{(i,1), \ldots, (i,Q)\}$ denotes quadratic arrays of $Q = 2 \times 2$ or 3×3 lattice sites, and the *product* potential

$$V_i(l) = V(l_{i,1}, \ldots, l_{i,Q}) = QU \prod_{q=1}^Q \theta(l_v - l_{i,q}), \quad (7)$$

which is equal to QU if $l_{i,q} \leq l_v$ for all q and vanishes otherwise. As *cis*-interactions, we now take hard-square interactions, i.e.,

$$W_{ij} = \infty \text{ for } j \text{ in } A_i^Q \text{ and zero otherwise}, \quad (8)$$

where A_i^Q denotes the exclusion area of an individual Q-sticker at lattice site i [17]. Stickers with the sum potential (6) and *cis*-interaction (8) correspond to quadratic clusters of 1×1 stickers since each lattice site (i,q) of a sticker interacts with the wall via a square-well potential of the form (2). The product potential (7) can be seen as a restriction of the binding conformation of large sticker molecules which only adhere to the wall if the sticker molecule has made Q local contacts.

It is instructive to ignore the hard-square interaction (8) for a moment and to study a Hamiltonian which is again linear in the concentration field n. For the product potential (7), a summation of the sticker degrees of freedom then again leads to an effective two-state membrane potential, which can be written as $V_i^{ef}(l) = U_{ef}\Pi_q \theta(l_v - l_{i,q})$ with $U_{ef} = -T \ln[(1 + e^{[\mu - QU]/T})/(1 + e^{\mu/T})] \equiv Tu_Q$. MC simulations of homogeneous membranes with this effective potential show a first order unbinding transition. In this case, we can explicitly calculate the effective line tension discussed in the introduction. Indeed, a quadratic cluster consisting of $L_o^2 Q$ stickers leads to a bound membrane segment of linear size $L = L_o + Q - 1$ and, thus, to a potential energy $QU(L - Q + 1)^2$, which involves the line tension $\Lambda = Q|U|2(Q - 1)$. Note that $\Lambda = 0$ for $Q = 1$. The sticker concentration $X = \langle n_i \rangle/a^2$ is now given by

$$X = \frac{1}{a^2} \left[(1 - P_{Qb})\frac{e^{\mu/T}}{1 + e^{\mu/T}} + P_{Qb} \frac{e^{[\mu - QU]/T}}{1 + e^{[\mu - QU]/T}} \right], \quad (9)$$

with $P_{Qb} \equiv \langle \Pi_q \theta(l_v - l_{i,q}) \rangle$. For $Q = 1$, we recover formula (5) with the contact probability $P_b = P_{1b}$. The phase diagrams can be obtained from MC results for the generalized contact probability P_{Qb} of the bound phase. In Fig. 4(a), we display the coexistence lines in the $(a^2 X, |U|/T)$–plane for $Q = 2 \times 2$ and $z_v = 0.1$. The sticker-poor phase for smaller X is unbound with $P_{Qb} = 0$.
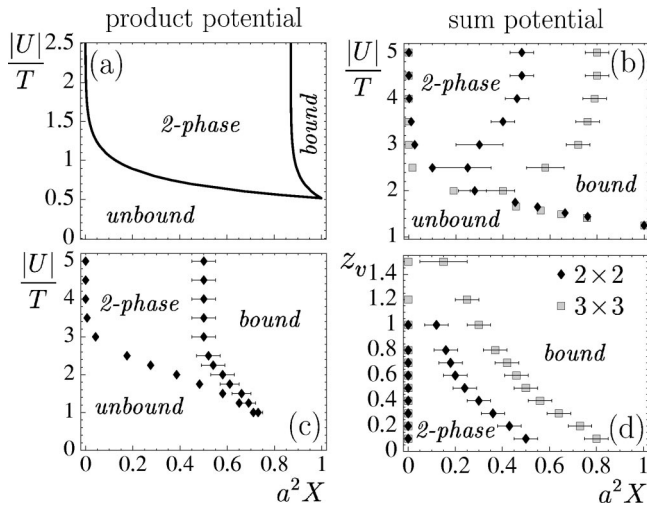
RAPID COMMUNICATIONS

FIG. 4. (Left column): Phase diagrams for quadratic stickers with *product* potential (7), size $Q = 2 \times 2$, and rescaled potential range $z_v = 0.1$; (a) without and (c) with the hard-square interaction (8). (Right column): Phase diagrams for stickers with *sum* potential (6), hard-square interaction, size $Q = 2 \times 2$ (black diamonds), and $Q = 3 \times 3$ (grey squares) at the rescaled potential range $z_v = 0.1$ in (b) and the reduced potential depth $|U|/T = 5$ in (d). The sticker concentration X is defined in the text.

Now we come back to the hard-square interaction (8). Figures 4(b) to 4(d) show phase diagrams from MC simulations with the sum potential (6) or the product potential (7) in the presence of the hard-square interaction (8). The sticker concentration X now is given by $Q \langle n_i \rangle / a^2$. At $z_v = 0.1$, the 2×2 and 3×3 stickers exhibit large coexistence regions; see Figs. 4(b) and 4(c). Since there are no attractive cis-

interactions, the phase separation is caused only by fluctuation-induced forces. In the case of stickers with the sum potential, as in Fig. 4(b), the unbinding transition is continuous for binding energies $|U|/T \lesssim 2$. The phase diagrams of 2×2 stickers with sum potential, shown in Fig. 4(b), and product potential as in Fig. 4(c) agree at high values of $|U|$ within the numerical accuracy since the majority of 2×2 stickers with the sum potential is then bound at all four lattice sites, thus resembling stickers with the product potential. The width of the coexistence regions decreases with increasing z_v [see Fig. 4(d)] as fluctuation effects become weaker. At high concentrations $X > 0.8/a^2$, the phase behavior is complicated by the packing transition of the hard-square lattice gas [18,19] which is not considered here [20].

In summary, both the adhesion and the phase behavior of multicomponent membranes is strongly affected by the relative size of the adhesive and the nonadhesive molecules. Adhesion molecules which occupy an area of Q nonadhesive membrane components lead (i) to phase separation within the adhering membrane, and (ii) to discontinuous unbinding transitions as shown explicitly for $Q = 4$ and $Q = 9$. For $Q = 1$, on the other hand, there is no phase separation (in the absence of attractive cis-interactions as studied here) and the corresponding unbinding transitions are continuous. These explicit results imply that the membrane behavior is changed as soon as the sticker size Q exceeds a threshold value Q_c with $1 \leq Q_c < 4$. In addition, our general arguments about the effective line tension arising from the interplay of shape fluctuations and sticker aggregation indicate that $Q_c = 1$.

Note added in proof. A different mechanism for adhesion-induced phase separation has been recently discussed by S. Komura and D. Andelman, Euro. Phys. J. E (to be published).

[1] R. Lipowsky, Curr. Opin. Struct. Biol. **5**, 531 (1995).
[2] E. Sackmann, in *The Structure and Dynamics of Membranes*, edited by R. Lipowsky and E. Sackmann (Elsevier, Amsterdam, 1995), pp. 213–304; P.F.F. Almeida and W.L.C. Vaz, *ibid.*, pp. 305–357.
[3] S.-W. Wu and H. McConnell, Biochemistry **14**, 847 (1975).
[4] P. Almeida, W. Vaz, and T. Thompson, Biochemistry **31**, 6739 (1992).
[5] J.L. Thewalt and M. Bloom, Biophys. J. **63**, 1176 (1992).
[6] M. Bloom and O.G. Mouritsen, in *The Structure and Dynamics of Membranes*, edited by R. Lipowsky and E. Sackmann (Elsevier, Amsterdam, 1995), pp. 65–95.
[7] S.L. Keller and H. McConnell, Phys. Rev. Lett. **82**, 1602 (1999).
[8] A.K. Hinderliter, J. Huang, and G.W. Feigenson, Biophys. J. **67**, 1906 (1994).
[9] R. Lipowsky, Phys. Rev. Lett. **77**, 1652 (1996).
[10] R. Lipowsky, Colloids Surf., A **128**, 255 (1997).
[11] J. Nardi, T. Feder, R. Bruinsma, and E. Sackmann, Europhys.

Lett. **37**, 371 (1997).
[12] A. Albersdörfer, T. Feder, and E. Sackmann, Biophys. J. **73**, 245 (1997).
[13] D. Braun and P. Fromherz, Phys. Rev. Lett. **81**, 5241 (1998).
[14] R.R. Netz, J. Phys. I **7**, 833 (1997).
[15] R. Lipowsky and S. Leibler, Phys. Rev. Lett. **56**, 2541 (1986); R. Lipowsky and B. Zielinska, *ibid.* **62**, 1572 (1989).
[16] The membrane size is assumed to be below the persistence length.
[17] We have also studied the case of 1×1 stickers with attractive cis-interactions $W_{ij} = W < 0$ as will be described elsewhere.
[18] L.K. Runnels, *Phase Transitions and Critical Phenomena*, edited by C. Domb and M.S. Green (Academic Press, New York, 1972), Vol. 2.
[19] W. Kinzel and M. Schick, Phys. Rev. B **24**, 324 (1981).
[20] Our model must also be distinguished from binary hard core mixtures characterized by *two* chemical potentials and depletion forces, see, e.g., D. Frenkel and A.A. Louis, Phys. Rev. Lett. **68**, 3363 (1992).